Modulation of Proton-Coupled Electron Transfer through Molybdenum-quinonoid Interactions

Justin T. Henthorn and Theodor Agapie*

Division of Chemistry and Chemical Engineering, California Institute of Technology, 1200 East California Boulevard, MC 127-72, Pasadena, California 91125, United States

*email: agapie@caltech.edu

Abstract

An expanded series of π -bound molybdenum-quinonoid complexes supported by pendant phosphines has been synthesized. These compounds formally span three protonation-oxidation states of the quinonoid fragment (catechol, semiquinone, quinone) and two different oxidation states of the metal (Mo⁰, Mo^{II}), notably demonstrating a total of two protons and four electrons accessible in the system. Previously, the reduced Mo⁰-catechol complex 1 and its reaction with dioxygen to yield the two-proton/two-electron oxidized Mo⁰-quinone compound 4 was explored, while herein the expansion of the series to include the two-electron oxidized Mo^{II}-catechol complex 2, the oneproton/two-electron oxidized Mo-semiquione complex 3, and the twoproton/four-electron oxidized Mo^{II}-quinone complexes 5 and 6 is reported. Transfer of multiple equivalents of protons and electrons from the Mo⁰ and Mo^{II} catechol complexes, 1 and 2, to H-atom acceptor TEMPO suggest the presence of weak O-H bonds. Although thermochemical analyses are hindered by the irreversibitiliy of the electrochemistry of the present compounds, the reactivity observed suggests weaker O-H bonds compared to the free catechol, indicating that proton-coupled electron transfer can be facilitated significantly by the π -bound metal center.

INTRODUCTION

Proton-coupled electron transfer (PCET) reactions are fundamental to some of the most complex and challenging transformations in small molecule conversion chemistry- namely multi-proton multi-electron processes. In biology, phenol and quinone moieties have been implicated in multi-electron processes, and as such the PCET of phenols and hydroquinones have been extensively studied in water, and to a lesser extent in non-aqueous solvents. Though π -bound transition metal quinonoid complexes have previously been reported, their study has largely focused on incorporation into metal-organometallic frameworks and thus their potential for PCET chemistry remains underexplored.

Noninnocent ligands supporting transition metals have been shown to facilitate storage or transfer of multiple redox⁷ or proton⁸ equivalents; however systems involving a single metal that can access multiple equivalents of both protons and electrons are quite rare. 15,9 Not only

could π -bound transition metal quinonoid complexes be envisioned to facilitate multi-proton, multi-electron transformations by accessing the protons and electrons stored in the quinonoid moiety, but also changes in the oxidation state at the metal center could be employed as a method to affect the PCET chemistry of the quinonoid fragment. We have recently reported the synthesis of a series of π -bound Mo 0 -quinonoid complexes and demonstrated their ability to transfer two H $^+$ (as well as R_2Si^{2+} , ArB^{2+} , and Me^+) and two electrons to $O_2.^{10}$ Herein we report an expanded series of Mo-quinonoid complexes in varying protonation and oxidation states spanning a total of two protons and four electrons, and investigate the impact of the metal-arene interaction on the PCET chemistry of the quinonoid fragment.

RESULTS AND DISCUSSION

Treatment of **1** with two equivalents of AgOTf in MeCN results in oxidation of the metal center by two electrons to yield the Mo^{II} complex **2** (Scheme 1). Oxidation of the metal center results in loss of a CO ligand and a haptotropic shift of the metal-arene interaction from η^2 to η^6 . Solution IR data for **2** in MeCN reveals strong bands assigned to carbonyl C–O stretches at 2010 and 1955 cm⁻¹ (ca. 250 cm⁻¹ higher in energy compared to **1**), consistent with a more oxidized metal center. A single crystal X-ray diffraction (XRD) study of **2** confirms the presence of the Mo(CO)₂ unit, but the crystal is highly disordered with respect to the two possible orientations of the catechol oxygen atoms throughout the lattice, thus hindering detailed discussion of the metal-arene interaction through bond metrics.

Treatment of **2** with one equivalent of 2,6-di-*tert*-butyl-4-methylpyridine (DTBMP) in MeCN results in quantitative monodeprotonation to yield **3**. The appearance of a band in the IR at 1608 cm⁻¹ and a carbon resonance in the ¹³C NMR spectrum at ca. 156 ppm are consistent with the formation of the semiquinone C=O moiety upon deprotonation. Additionally, a shift to lower energy of the IR bands assigned to Mo-bound carbon monoxide C–O stretches (1904 and 1880 cm⁻¹ in **3**) is consistent with a more electron rich metal center, as has also been previously observed in cationic Mn(CO)₃ quinonoid complexes.¹¹ An XRD study of **3** (Figure 1) confirms these spectroscopic findings, revealing one long quinonoid C–O bond (avg 1.33 Å) and one short quinonoid C–O bond (avg 1.26 Å), consistent with the (formally) semiquinone assignment. Compound **3** can be

further deprotonated with Et_3N to yield the previously reported compound ${f 4}.$

Scheme 1. Synthesis and reactivity of Mo-quinonoid complexes

Reaction of 4 with two equivalents of AgOTf in a 1:1 mixture of THF/MeCN results in the formation of two isomers, as determined by ³¹P NMR spectroscopy and crystallography (Fig 1), differing in the position of the CO ligand relative to the quinone moiety. The major species **5a**, which resonates as a singlet at ca. 75 ppm in CD₃CN (³¹P), can be enriched to approximately 80% via successive recrystallizations, albeit in low yield (~20%). XRD studies of **5a** and **5b** reveal Mo^{II}quinone complexes with two outer-sphere counter anions. Oxidation of the metal center from (formally) Mo⁰ to Mo^{II} results in loss of a carbonyl ligand and coordination of two MeCN molecules, yielding a pseudo-pentagonal bipyramidal geometry about the metal center with the remaining carbonyl anti with respect to the quinone oxygens for 5a and syn for **5b**. Upon oxidation the quinone fragment retains the short C-O bonds (avg 1.22 Å in **5a** and **5b** compared to 1.23 Å in **4**), while the diene fragment reveals a slight contraction of the C=C bonds (avg 1.41 Å in **5a** and **5b** compared to 1.44 Å in **4**) consistent with less π backbonding in the more oxidized complex. The syntheses of compounds 4 and 5a/5b described above involve sequential steps involving the separate transfer of 2e and 2H. These compounds can also be prepared in single synthetic steps from 1 via reaction with 2 equivalents of 2,4,6-tri-tert-butylphenoxy radical and from 2 via reaction with 2,3dichloro-5,6-dicyano-1,4-benzoquinone (DDQ), respectively, in combined 2e⁻/2H⁺ transformations.

Oxidation of **4** with PhICl₂ results in formation of a third Mo^{II}-quinone complex **6**. Here again a CO ligand is lost upon oxidation and binding of two chloride ligands and a single isomer is generated (NMR and IR spectroscopy). An XRD study (Fig 1) shows the CO ligand *syn* with respect to the quinone CO moieties (analogous to **5b**) and bond metrics similar to those of **5a** and **5b**. Compounds **5a**, **5b**, and **6** represent rare examples of accessing redox equivalents beyond the two stored in the catechol moiety, and allow two different oxidation state entries into the study of PCET chemistry of Mo-quinonoid complexes.

Reactions of compounds 1 and 2 with (2,2,6,6-tetramethylpiperidyl)oxyl (TEMPO) were performed in MeCN (Scheme 2). Compound 1 reacts with TEMPO to quantitatively yield 4, while 2 yields a mixture of 5 and 4 in ca. 1:1 ratio (¹H NMR spectroscopy). The formation of both oxidized (compound 5) and deprotonated (compounds 3 and 4) products from the reactions of compound 2 with TEMPO can be rationalized via competing acid-base side reactions between 2 and the by-product TEMPOH. As a control, under identical conditions it was found that the metal-free catechol compound 2,6-bis(orthobromophenyl)catechol (8) exhibited no reaction with TEMPO, while the corresponding quinone 11 does react with TEMPOH to generate 8.

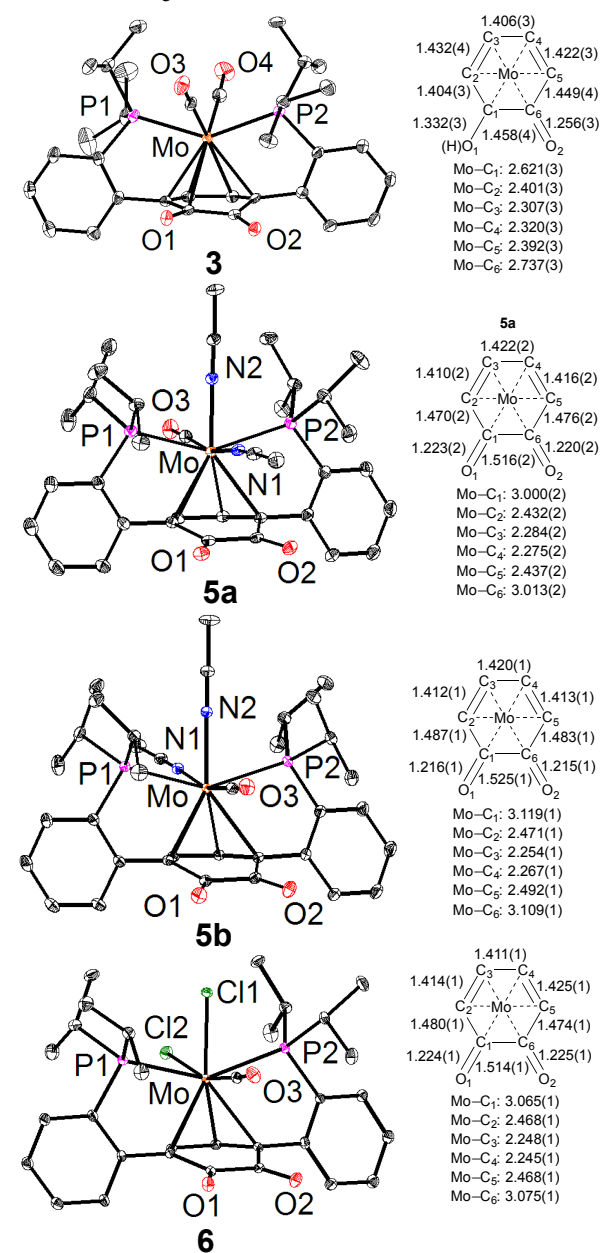


Figure 1. Solid-state structures of **3**, **5a**, **5b** and **6** with 50% probability thermal ellipsoids. Solvent molecules, hydrogen atoms, and outer-sphere anions are omitted for clarity. Carbon atoms are depicted in black. Select bond distances (average values of four molecules in asymmetric unit for **3**) are given in Å.

Scheme 2. Reactivity of quinonoid complexes with TEMPO

These results suggest that the O-H bonds in compounds 1 and 2 are relatively weak, as they react with TEMPO to generate TEMPOH, with a reported O-H BDFE of 66.5 kcal/mol (in MeCN).¹³ Furthermore, the metal-quinonoid complexes are activated with respect to (overall) H-atom transfer when compared to the metal-free compound 8. Species 8 shows no reactivity with TEMPO under similar conditions, while the corresponding quinone (11, see SI) does react with TEMPOH, demonstrating that the O-H bond in TEMPOH is weaker than in 8. Based on these reactions alone, thermodynamic assumptions cannot be made about the Mo complexes, as CO is irreversibly lost upon oxidation. BDFE's for the first O-H could be calculated from the pK_a's of compounds 1, 2, and 3 and the oxidation potentials of the respective conjugate bases using equation 1.^{1b}

BDFE_{MeCN}(X-H) =
$$54.9 + 1.37$$
pK_a(X-H/X⁻) + 23.06 E°(X⁻/X[•]) (1)

The pK_a's for compounds 1 (25.89(9)), 2 (4.74(9)), 3 (17.1(4)), and $8\ (26.3(1))$ were determined in MeCN using acids/bases of known strength, measuring the equilibrium constants by ¹H NMR spectroscopy (see supplementary information for further details) and combining the equilibrium constant with the pKa of the known acid/base using Hess's Law to determine the pKa of the desired compounds as previously reported.¹⁴ The conjugate bases of compounds 2 and 3 are compounds 3 and 4, respectively, and their preparations found above and elsewhere,10 while the conjugate bases of 1 and 8 were prepared via deprotonation with benzyl potassium in the presence of crown ether (see supplementary information). Oxidation potentials were determined via electrochemical experiments (Figure 2). In all cases, two oxidation events¹⁵ were observed via cyclic and square-wave voltammetries, with the first event being the one necessary for calculation of BDFEs. Unfortunately, all observed events were irreversible, with the exception of the first event for the conjugate base of 8 (purple traces, Figure 2). Since oxidation potentials determined from irreversible redox events are not thermodynamic potentials, they cannot be used to rigorously calculate BDFEs. While phenolic BDFE values have previously been calculated using irreversible oxidation events measured via cyclic voltammetry, 1b,16 in those cases, chemically similar compounds were compared. The irreversible oxidation potentials measured here will be used for a qualitative discussion (see SI for estimates of BDFEs using eq 1).

Comparing first compound 1 to compound 8, the effect of η^2 coordination of the Mo⁰(CO)₃ moiety to the quinonoid fragment on the

PCET transfer can be evaluated. Compound ${\bf 1}$ and ${\bf 8}$ exhibit similar pK_a values (25.89(9) and 26.3(1)), while the presence of the Mo⁰(CO)₃ unit in ${\bf 1}$ shifts the irreversible oxidation potential 140 mV more negative, both in the direction of a weaker O–H bond (eq 1) for ${\bf 1}$ consistent with the TEMPO reactivity.

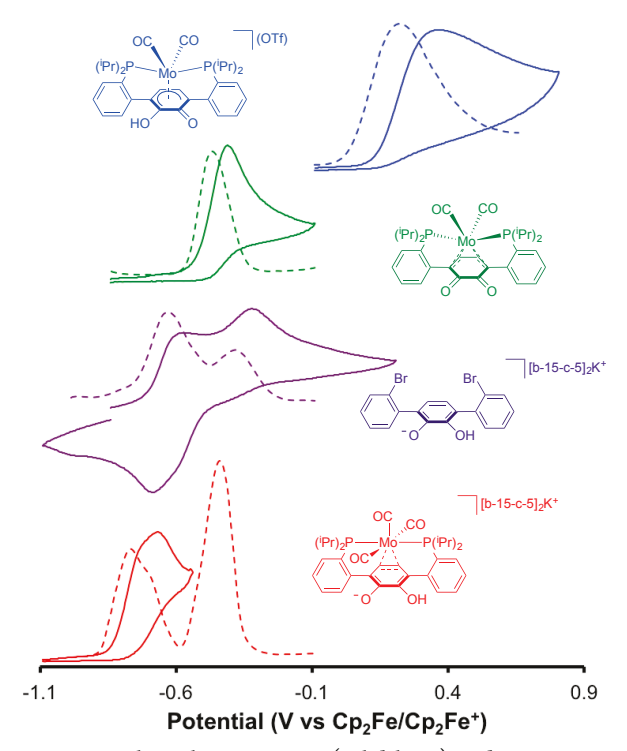


Figure 2. Cyclic voltammograms (solid lines) and square-wave voltammograms (dashed lines) of conjugate bases of compounds **1** (red), **2** (blue), **3** (green), and **8** (purple) in 0.1 M [n Bu₄N⁺][PF₆⁺] in MeCN recorded with a glassy carbon electrode. Scan rate of 50 mV/s for cyclic voltammograms. (b-15-c-5) = benzo-15-crown-5.

Next, comparing compound **1** to compound **2**, the effect of changing the oxidation state of the metal center on the PCET chemistry can be analyzed. Oxidation of **1** from Mo⁰ to Mo^{II} accompanied by loss of a CO ligand and a shift of the metal-quinonoid interaction from η^2 to η^6 results in >20 orders of magnitude increase in acidity, with a measured pK_a of 4.74(9) for **2** compared to 25.89(9) for **1**. This increase in acidity is greater than the calculated increase in acidity for phenol upon one-electron oxidation.¹⁷ The oxidation from **1** to **2** also results in a large positive shift in the irreversible oxidation potential of the conjugate base (+0.220 V for conjugate base of **2** compared to -0.770 V for conjugate base of **1**), consistent with a more electron deficient species. Compared to **8**, the increased acidity in **2** thermodynamically outweighs the positive shift in oxidation potential given the reactivity with TEMPO.

The effect of protonation state while maintaining the same overall oxidation state on the metal-quinonoid interaction on the resulting PCET chemistry can be analyzed by comparing compounds **2** and **3**. Deprotonation of **2** to yield **3** results in a shift of the metal-quinonoid interaction from η^6 to η^5 , as well as a decrease in the overall charge from di-cation to mono-cation. The acidity of the remaining O–H moiety (pK_a = 17.1(4)) of **3**, is significantly lower than in **2**. A more negative irreversible oxidation potential of the conjugate base (-0.470 V) is observed for **3**.

These results demonstrate that metal-quinonoid interactions can be used to modulate the PCET of the quinonoid fragment, as indicated by

the increased reactivity with TEMPO compared to catechol 8. Not only does the strength of the O-H bond weaken with increasing metalquinonoid interaction, but changes in the acidity and irreversible oxidation potentials could result in access to different PCET pathways. For example, compound 1 exhibits relatively low acidity ($pK_a = 25.89(9)$) and mild reducing power (E°_{Irr} = -0.285 V), with a significant shift in the irreversible oxidation potential upon proton transfer ($E^{\circ}_{Irr} = -0.770$ V for the conjugate base). These thermodynamic parameters suggest that compound 1 is likely to proceed through either a concerted proton-electron transfer (CPET) pathway or a stepwise electron transferproton transfer (ET-PT) pathway, and disfavors the stepwise PT-ET pathway. Alternatively, compound 2 exhibits significantly greater acidity (pK_a = 4.74(9)) and low reducing power (E°_{Irr} = +0.94 V), with a large shift in oxidation potential upon proton transfer ($E^{\circ}_{Irr} = +0.220 \text{ V}$ for conjugate base 3). These thermodynamic parameters suggest compound 2 is likely to proceed through a CPET pathway or a stepwise PT-ET pathway, and disfavors a stepwise ET-PT pathway.

CONCLUSION

In summary, the synthesis of an expanded series of Mo-quinonoid complexes has been reported, demonstrating a total of two protons and four electrons accessible to the system. The Mo⁰-catechol and Mo^{II}-catechol complexes both exhibit PCET reactivity with TEMPO, in contrast with the reactivity of metal free catechol 8. Qualitatively, the η^2 interaction of the Mo⁰(CO)₃ moiety with the catechol in 1 as well as the η^6 interaction of the Mo⁰(CO)₂ moiety with the catechol in 2 results in a decrease in the BDFE of O–H as compared to the metal-free catechol 8. Furthermore, changing the oxidation state of the metal center from Mo⁰ to Mo^{II} may allow access to alternate PCET pathways based on changes in acidities and irreversible oxidation potentials. These results prompt further investigation into the use of π -bound transition metal fragments to modulate the PCET chemistry of hydroquinone and other similar moieties within the context of multi-proton multi-electron small molecule transformations.

EXPERIMENTAL SECTION

General considerations: Unless indicated otherwise, reactions performed under inert atmosphere were carried out in oven-dried glassware in a glovebox under a nitrogen atmosphere purified by circulation through RCI-DRI 13X-0408 Molecular Seives 13X, 4x8 Mesh Beads and BASF PuriStar® Catalyst R3-11G, 5x3 mm (Research Catalysts, Inc.). Solvents for all reactions were purified by Grubbs' method. 18 CD₃CN and CD₂Cl₂ were purchased from Cambridge Isotope Laboratories and distilled from CaH2 prior to use. Alumina and Celite were activated by heating under vacuum at 200 °C for 24 hours. 1H, 19F, and ³¹P NMR spectra were recorded on Varian Mercury 300 MHz spectrometers at ambient temperature, unless denoted otherwise. ¹³C NMR spectra were recorded on a Varian INOVA-500 MHz spectrometer. ¹H and ¹³C NMR chemical shifts are reported with respect to internal solvent: 1.94 ppm and 118.26 for CD₃CN, and 5.32 ppm and 53.84 ppm for CD₂Cl₂, respectively. ¹⁹F and ³¹P NMR chemical shifts are reported with respect to an external standard of C₆F₆ (-164.9 ppm) and $85\% H_3PO_4$ (0.0 ppm).

Powder and thin film ATR-IR measurements were obtained by placing a powder or drop of solution of the complex on the surface of a Bruker APLHA ATR-IR spectrometer probe and allowing the solvent to evaporate (Platinum Sampling Module, diamond, OPUS software package) at 2 cm $^{-1}$ resolution. Solution IR spectra were recorded on a Thermo-Fisher Scientific Nicolet 6700 FTIR spectrometer using a CaF2 plate solution cell.

Unless otherwise noted all chemical reagents were purchased from commercial sources and used without further purification. AgOTf, 2,3-

dichloro-5,6-dicyano-1,4-benzoquinone and benzo-15-crown-5 were purchased from Sigma Aldrich and used as received. 2,6-di-*tert*-butyl-4-methylpyridine, 4-*tert*-butylphenol, 2-nitroaniline, and [2,2,2]-diazobicyclooctane were purchased from Sigma Aldrich and sublimed prior to use. PhICl₂, 19 1, 10 4, 10 and 8 10 were prepared using literature procedures.

Synthesis [1,4-bis(2-(diisopropylphosphino)phenyl)-2,3-catechol] dicarbonylmolybdenum(II) bis(trifluoromethanesulfonate) (2) Compound 1 (0.0833 g, 0.123 mmol) was stirred as a suspension in MeCN (2 mL). AgOTf (0.0617 g, 0.240 mmol) was added as a solution in MeCN (2 mL) to the stirring suspension. Upon addition the reaction became a purple heterogeneous mixture, which was stirred at room temperature until the purple color dissipated (approximately 20 min), resulting in a yellow/brown heterogeneous mixture. The solution was then filtered through celite and the filtrate evaporated under reduced pressure. The resulting residue was freed of excess MeCN by trituration with hexanes (3 mL), followed by evaporation under reduced pressure to yield a tan solid (0.1089 g, 93%). 1H NMR (500 MHz, CD₃CN, 25 °C): δ 10.07 (s, 2 H, Ar-OH), 7.87 (m, 4 H), 7.80 (t, 7.5 Hz, 2 H), 7.77 (t, 7 Hz, 2 H), 6.46 (s, 2H), 3.32 (m, 2 H, $CH(CH_3)_2$). 3.20 (m, 2 H, $CH(CH_3)_2$), 1.37 (m, 6 H, $CH(CH_3)_2$), 1.31 (m, 6 H, $CH(CH_3)_2$), 1.21 (m, 6 H, $CH(CH_3)_2$), 1.18 (m, 6 H, CH(CH₃)₂). ³¹P NMR (121 MHz, CD₃CN, 25 °C): 72.38 (s). ¹⁹F NMR (282 MHz, CD₃CN, 25 °C): -79.33 (s). ¹³C NMR (150 MHz, CD₃CN, 25 °C): 226.99 (t, Mo-CO), 224.17 (t, Mo-CO), 140.34 (s, Ar-C), 137.96 (m, Ar-C), 136.49 (m, Ar-C), 134.62 (s, Ar-C), 134.28 (s, Ar-C), 131.94 (t, Ar-C), 129.89 (t, Ar-C), 124.87 (t, Ar-C), 95.74 (s, Ar-C), 28.83 (m, $CH(CH_3)_2$), 18.58 (s, $CH(CH_3)_2$), 18.00 (s, $CH(CH_3)_2$), 17.92 (s, $CH(CH_3)_2$). IR (MeCN), v_{CO} (cm⁻¹): 2010, 1955. Anal. Calcd for [2], C₃₄H₄₀F₆MoO₁₀P₂S₂: C, 43.23; H, 4.27. Found: C, 43.16; H, 4.38.

[1,4-bis(2-Synthesis (diisopropylphosphino)phenyl)-2,3semiquinonate]dicarbonylmolybdenum(II) trifluoromethanesulfonate (3) To a solution of 1 (0.0427 g, 0.0452 mmol) in MeCN (2 mL) was added 2,6-di-tert-butyl-4-methylpyridine (0.0049 g, 0.0437 mmol) as a solution in MeCN (2 mL). The mixture was stirred at room temperature for 30 minutes, at which point the volatiles were removed under vacuum. The resulting residue was taken up in a minimal amount of MeCN and added to a stirred solution of Et₂O (15 mL) drop-wise. Upon complete addition, the resulting suspension was cooled to -35 °C for 20 minutes and then filtered cold on a pad of celite. The solid was dissolved in MeCN, filtered, and concentrated under vacuum to afford the desired product (0.0258 g, 72%). Crystals suitable for X-ray diffraction were grown via vapor diffusion of Et₂O into a saturated solution of 3 in DMF. ¹H NMR (300 MHz, CD₃CN, 25 °C): δ 9.09 (s, br), 7.77 (m, 4 H), 7.68 (m, 4H), 5.90 (s, 2 H), 3.17 (m, 4 H), 1.28 (m, 18 H), 1.06 (m, 6 H). ³¹P NMR (121 MHz, CD₃CN, 25 °C): 72.02 (s). ¹⁹F NMR (282 MHz, CD₃CN, 25 °C): -79.19 (s). ¹³C NMR (150 MHz, CD₃CN, 25 °C): 236.68 (t, Mo-CO), 229.21 (t, Mo-CO), 156.00 (s, Ar-C), 142.65 (t, Ar-C), 136.55 (m, Ar-C), 133.38 (s, Ar-C), 133.10 (s, Ar- C_6), 130.10 (s, Ar-C), 129.88 (s, Ar-C), 116.70 (s, Ar-C), 88.92 (s, Ar-C₃), 28.89 (t, $CH(CH_3)_2$), 27.33 (t, $CH(CH_3)_2$), 18.43 (s, $CH(CH_3)_2$), 18.24 (s, $CH(CH_3)_2$), 18.04 (s, $CH(CH_3)_2$). IR (THF, cm⁻¹), v_{CO} : 1904, 1880, 1608. Anal. Calcd for [3], C₃₃H₃₉F₃MoO₇P₂S: C, 49.88; H, 4.95. Found: C, 49.56; H, 5.02.

Synthesis of [1,4-bis(2-(diisopropylphosphino)phenyl)-2,3-benzoquinone]bis(acetonitrile)carbonylmolybdenum(II) trifluoromethanesulfonate (5a and 5b) Compound 2 (3.0274 g, 3.20 mmol) and 2,3-dichloro-5,6-dicyano-1,4-benzoquinone

(0.7187 g, 3.17 mmol) were combined in a schlenk tube charged with a stir bar and MeCN (15 mL). The schlenk tube was sealed and heated to 80 °C for 3 hours. Completion of the reaction was determined via ³¹P NMR analysis of an aliquot of the reaction mixture, revealing loss of the starting material at \sim 72 ppm, and presence of two new signals at ca. 74 ppm and ca. 70 ppm. After cooling to room temperature, all volatiles were removed under vacuum. The residue was then vigorously triturated with THF (8 mL) to precipitate a brick red powder, and the solid collected on a glass frit. The solid was then redissolved in a minimal amount of MeCN and recrystallized via vapor diffusion of Et₂O. Crystals grown from this mixture after 48 hours at room temperature were then collected and dried under vacuum to afford a mixture of 5a and **5b** in ca. 3:2 ratio (2.6323 g, 82%). These crystals were found suitable for X-ray diffraction. Note: the NCCH3 ligands exchange slowly with the CD₃CN NMR solvent for compound 5b, such that the bound acetonitrile can be easily observed by both ¹H and ¹³C NMR spectroscopies. Compound **5a** exhibits faster ligand exchange, such that signals for the bound acetonitrile ligands could only be observed by ¹H NMR spectroscopy.

5a: ¹H NMR (300 MHz, CD₃CN, 25 °C), δ (ppm): 7.6 – 7.8 (m, 8 H, Ar-C*H*), 6.22 (t, J_{PH} = 1.4 Hz, 2 H, Ar-C*H*), 3.49 (m, 2 H, PC*H*(CH₃)₂), 3.14 (m, 2 H, PC*H*(CH₃)₂), 3.10 (t, 3.6 Hz, 3 H, equatorial NCC*H*₃), 2.48 (s, 3 H, axial NCC*H*₃), 1.2 – 1.5 (m, 18 H, PCH(C*H*₃)₂), 0.70 (m, 6 H, PCH₂(C*H*₃)₂). ³¹P NMR (121 MHz, CD₃CN, 25 °C), δ (ppm): 74.63 (s). ¹⁹F NMR (282 MHz, CD₃CN, 25 °C): -79.22 (s). ¹³C NMR (125 MHz, CD₃CN, 25 °C), δ (ppm): 213.38 (t, Mo-CO), 178.73 (s, Ar-C), 147.06 (t, Ar-C), 143.00 (t, Ar-C), 135.31 (s, Ar-C), 133.36 (t, Ar-C), 132.15 (s, Ar-C), 131.92 (t, Ar-C), 130.91 (t, Ar-C), 88.79 (s, Ar-C), 29.54 (m, PCH(CH₃)₂), 27.53 (t, PCH(CH₃)₂), 20.82 (s, PCH(CH₃)₂), 20.27 (s, PCH(CH₃)₂), 19.71 (t, PCH(CH₃)₂), 18.75 (t, PCH(CH₃)₂). IR (powder), ν _{CO} (cm⁻¹): 2020, 1680.

5b: ¹H NMR (300 MHz, CD₃CN, 25 °C), δ (ppm): 7.6 – 7.8 (m, 8 H, Ar-CH), 6.27 (t, J_{PH} = 1.2 Hz, 2 H, Ar-CH), 3.49 (m, 2 H, PCH(CH₃)₂), 3.32 (m, 2 H, PCH(CH₃)₂), 2.98 (t, 3.6 Hz, 3 H, equatorial NCCH₃), 2.57 (s, 3 H, axial NCCH₃), 1.2 – 1.5 (m, 12 H, PCH(CH₃)₂), 1.09 (m, 6 H, PCH₂(CH₃)₂), 1.04 (m, 6 H, PCH₂(CH₃)₂). ³¹P NMR (121 MHz, CD₃CN, 25 °C), δ (ppm): 70.25 (s). ¹⁹F NMR (282 MHz, CD₃CN, 25 °C): -79.22 (s). ¹³C NMR (125 MHz, CD₃CN, 25 °C), δ (ppm): 219.05 (t, Mo-CO), 175.53 (s, Ar-C), 144.34 (t, Ar-C), 142.26 (t, Ar-C), 130.91 (t, Ar-C), 92.96 (s, Ar-C), 30.61 (m, PCH(CH₃)₂), 27.87 (t, PCH(CH₃)₂), 20.37 (s, PCH(CH₃)₂), 20.27 (s, PCH(CH₃)₂), 19.74 (s, PCH(CH₃)₂), 18.65 (t, PCH(CH₃)₂). IR (powder), v_{Co} (cm⁻¹): 1990, 1680. Anal. Calcd for [**5a/5b**] • MeCN, C₃₉H₄₇F₆MoN₃O₉P₂S₂: C, 45.14; H, 4.56; N, 4.05. Found: C, 45.34; H, 4.61; N, 4.04.

Synthesis of [1,4-bis(2-diisopropylphosphino)phenyl)-2,3-

benzoquinone]dichlorocarbonylmolybdenum(II) (6) In the glovebox, a schlenk flask was charged with compound 4 (0.1712 g, 0.234 mmol), MeCN (10 mL), and a stir bar, and the flask was brought out to the schlenk line. Under a counterflow of N₂, PhICl₂ (0.1505 g, 0.547 mmol) was added all at once as a solid. The reaction became a dark red homogeneous solution with evolution of gas. The reaction was stirred under N₂ for 1 hour at room temperature, during which a large amount of brick-red material had precipitated from solution. The volatiles were then removed under reduced pressure and the schlenk flask then returned to the glovebox. The residue was triturated with THF (20 mL) and the precipitate collected on a glass frit, washing with additional THF (10 mL). The solid was then dried under vacuum to afford the desired product as a brick-red powder in 87.5% yield (0.6621

g). Crystals suitable for X-ray diffraction were grown via layering of pentane onto a saturated solution of the compound in DCM. 1 H NMR (300 MHz, CD₂Cl₂ , 25 °C), δ (ppm): 7.62 (m, 4 H, Ar-CH), 7.55 (m, 2 H, Ar-CH), 7.47 (m, 2 H, Ar-CH), 7.45 (m, 2 H, Ar-CH), 5.93 (s, Ar-CH), 3.57 (m, 2 H, PCH(CH₃)₂), 3.13 (m, 2 H, PCH(CH₃)₂), 1.57 (m, 6H, PCH(CH₃)₂), 1.48 (m, 6H, PCH(CH₃)₂), 1.27 (m, 6H, PCH(CH₃)₂), 0.55 (m, 6 H, PCH(CH₃)₂). 31 P NMR (121 MHz, CD₂Cl₂ , 25 °C), δ (ppm): 53.48 (s). 13 C NMR (125 MHz, C₆D₆ , 25 °C), δ (ppm): 220.88 (t, Mo-CO), 174.96 (s, Ar-C), 143.58 (t, Ar-C), 133.90 (t, Ar-C), 130.98 (s, Ar-C), 130.91 (t, Ar-C), 129.97 (s, Ar-C), 129.74 (t, Ar-C), 115.29 (t, Ar-C), 94.67 (s, Ar-C), 29.78 (t, PCH(CH₃)₂), 27.10 (t, PCH(CH₃)₂), 20.60 (t, PCH(CH₃)₂), 20.26 (t, PCH(CH₃)₂), 19.83 (t, PCH(CH₃)₂), 18.84 (m, PCH(CH₃)₂), 16.34. IR (powder), v_{Co} (cm⁻¹): 1965, 1652. Anal. Calcd for [**6**], C₃₁H₃₈MoO₃P₂: C, 54.16; H, 5.57. Found: C, 53.40; H, 5.54.

ASSOCIATED CONTENT

Supporting Information

Experimental procedures, spectroscopic data and crystallographic details (CIF). This material is available free of charge via the Internet at http://pubs.acs.org.

AUTHOR INFORMATION

Corresponding Author

*Email: agapie@caltech.edu

Notes

The authors declare no competing financial interests.

ACKNOWLEDGMENTS

We thank Lawrence M. Henling and Dr. Michael Takase for crystallographic assistance and Choon Heng (Marcus) Low for synthesizing quinone 11 and for performing some of the control experiments. We thank Caltech and the NSF (CHE-1151918, T.A., and NSF GRFP, J.T.H.) for funding. TA is grateful for Sloan, Cottrell, and Dreyfus fellowships. The Bruker KAPPA APEXII X-ray diffractometer was purchased via an NSF CRIF:MU award to Caltech, CHE-0639094.

REFERENCES

- (1) (a) Weinberg, D. R.; Gagliardi, C. J.; Hull, J. F.; Murphy, C. F.; Kent, C. A.; Westlake, B. C.; Paul, A.; Ess, D. H.; McCafferty, D. G.; Meyer, T. J. *Chem. Rev.* **2012**, *112*, 4016-4093. (b) Warren, J. J.; Tronic, T. A.; Mayer, J. M. *Chem. Rev.* **2010**, *110*, 6961-7001.
- (2) (a) Stubbe, J.; Nocera, D. G.; Yee, C. S.; Chang, M. C. Y. Chem. Rev. 2003, 103, 2167-2202. (b) Whittaker, J. W. Chem. Rev. 2003, 103, 2347-2364.
- (3) (a) Barber, J. Inorg. Chem. 2008, 47, 1700-1710.
 (b) Meyer, T. J.;
 Huynh, M. H. V.; Thorp, H. H. Angew. Chem. Int. Ed. 2007, 46, 5284-5304.
 (c) Osyczka, A.; Moser, C. C.; Dutton, P. L. Trends Biochem. Sci. 2005, 30, 176-182.
- (4) (a) DeFelippis, M. R.; Murthy, C. P.; Broitman, F.; Weinraub, D.; Faraggi, M.; Klapper, M. H. *J. Phys. Chem.* **1991**, *95*, 3416-3419. (b) Harriman, A. *J. Phys. Chem.* **1987**, *91*, 6102-6104. (c) Jovanovic, S. V.; Harriman, A.; Simic, M. G. *J. Phys. Chem.* **1986**, *90*, 1935-1939.
- (5) (a) Hui, Y.; Chng, E. L. K.; Chng, C. Y. L.; Poh, H. L.; Webster, R. D. *J. Am. Chem. Soc.* **2009**, *131*, 1523-1534. (b) Quan, M.; Sanchez, D.; Wasylkiw, M. F.; Smith, D. K. *J. Am. Chem. Soc.* **2007**, *129*, 12847-12856.
- (6) (a) Kim, S. B.; Pike, R. D.; Sweigart, D. A. Acc. Chem. Res. 2013, 46, 2485-2497. (b) Moussa, J.; Amouri, H. Angew. Chem. Int. Ed. 2008, 47, 1372-1380. (c) Reingold, J. A.; Uk Son, S.; Bok Kim, S.; Dullaghan, C. A.; Oh, M.; Frake, P. C.; Carpenter, G. B.; Sweigart, D. A. Dalton Trans. 2006, 2385-2398.
- (7) (a) Luca, O. R.; Crabtree, R. H. Chem. Soc. Rev. 2013, 42, 1440-1459.
 (b) Lyaskovskyy, V.; de Bruin, B. ACS Catalysis 2012, 2, 270-279.
 (c) Praneeth, V. K. K.; Ringenberg, M. R.; Ward, T. R. Angew. Chem. Int. Ed. 2012, 51, 10228-10234.
 (d) Eisenberg, R.; Gray, H. B. Inorg. Chem. 2011, 50, 9741-9751.
 (e) Chirik, P. J.; Wieghardt, K. Science 2010, 327, 794-795.
- (8) (a) Nadif, S. S.; O'Reilly, M. E.; Ghiviriga, I.; Abboud, K. A.; Veige, A. S. Angew. Chem. Int. Ed. 2015, 54, 15138-15142. (b) Umehara, K.; Kuwata, S.; Ikariya, T. J. Am. Chem. Soc. 2013, 135, 6754-6757. (c) Carver, C. T.; Matson, B. D.; Mayer, J. M. J. Am. Chem. Soc. 2012, 134, 5444-5447. (d) Costentin, C.; Drouet, S.; Robert, M.; Savéant, J.-M. Science 2012, 338, 90-94. (e) Hull, J. F.; Himeda, Y.; Wang, W.-H.; Hashiguchi, B.; Periana, R.; Szalda, D. J.; Muckerman, J. T.; Fujita, E. Nat Chem 2012, 4, 383-388. (f) Gunanathan, C.; Milstein, D. Acc. Chem. Res. 2011, 44, 588-602. (g) Kohl, S. W.; Weiner, L.; Schwartsburd, L.; Konstantinovski, L.; Shimon, L. J. W.; Ben-David, Y.; Iron, M. A.; Milstein, D. Science 2009, 324, 74-77. (h) Rakowski, M.; DuBois, D. L. Chem. Soc. Rev. 2009, 38, 62-72.
- (9) (a) Thompson, E. J.; Berben, L. A. Angew. Chem. Int. Ed. 2015, 54, 11642-11646. (b) Lu, F.; Zarkesh, R. A.; Heyduk, A. F. Eur. J. Inorg. Chem. 2012, 2012, 467-470. (c) Purse, B. W.; Tran, L.-H.; Piera, J.; Åkermark, B.; Bäckvall, J.-E. Chem. Eur. J. 2008, 14, 7500-7503. (d) Collman, J. P.; Devaraj, N. K.; Decréau, R. A.; Yang, Y.; Yan, Y.-L.; Ebina, W.; Eberspacher, T. A.; Chidsey, C. E. D. Science 2007, 315, 1565-1568. (e) Chang, C. J.; Chng, L. L.; Nocera, D. G. J. Am. Chem. Soc. 2003, 125, 1866-1876. (f) Chaudhuri, P.; Hess, M.; Müller, J.; Hildenbrand, K.; Bill, E.; Weyhermüller, T.; Wieghardt, K. J. Am. Chem. Soc. 1999, 121, 9599-9610.
- (10) Henthorn, J. T.; Lin, S.; Agapie, T. J. Am. Chem. Soc. 2015, 137, 1458-1464.
- (11) Oh, M.; Carpenter, G. B.; Sweigart, D. A. Organometallics 2002, 21, 1290-1295.
- (12) Mader, E. A.; Manner, V. W.; Markle, T. F.; Wu, A.; Franz, J. A.; Mayer, J. M. J. Am. Chem. Soc. **2009**, *131*, 4335-4345.
- (13) Zhao, Y.; Bordwell, F. G.; Cheng, J.-P.; Wang, D. J. Am. Chem. Soc. 1997, 119, 9125-9129.
- (14) Teets, T. S.; Labinger, J. A.; Bercaw, J. E. Organometallics 2013, 32, 5530-5545.
- (15) Both oxidation events are shown for the purple and red traces in Figure 2. In the blue and green traces, the second event was further removed from the first, and thus have been omitted for clarity.
 - (16) Bordwell, F. G.; Cheng, J. J. Am. Chem. Soc. 1991, 113, 1736-1743.
- (17) Koo, B. J.; Huynh, M.; Halbach, R. L.; Stubbe, J.; Nocera, D. G. *J. Am. Chem. Soc.* **2015**, *137*, 11860-11863.
- (18) Pangborn, A.B.; Giardello, M.A.; Grubbs, R.H.; Rosen, R.K.; Timmers, F.J. Organometallics 1996, 15, 1518-1520.
 - (19) Podgorsek, A.; Iskra, J. Molecules 2010, 15, 2857–2871.

For Table of Contents Only:



A series of π -bound molybdenum-quinonoid complexes provides access to a total of two protons and four electrons in the system. Analysis of acid-base and redox chemistry reveals a significant shift in the reactivity of the O–H moieties compared to related metal free catechols, demonstrating that proton-coupled electron transfer can be facilitated significantly by the π -bound metal center.